

Investigation of Zone and Type of Scaling Based on the Fluid Flow Pattern in the Geothermal Well “X” at the Salak Geothermal Field - Indonesia

Akhmad Sofyan^{*,**‡} , János Szanyi^{*} , Hari Sumantri Aka^{**} 

^{*}Department of Mineralogy, Geochemistry and Petrology, Faculty of Earth Science, University of Szeged, 13 Dugonics Square Szeged 6722, Hungary

^{**}Polytechnic of Energy and Mineral Akamigas, Ministry of Energy and Mineral Resources (KESDM), Cepu, Central Java, Blora, 58315, Indonesia

(akhmad.sofyan@geo.u-szeged.hu, szanyi@iif.u-szeged.hu, harisumantriaka@gmail.com)

[‡]Corresponding Author; Akhmad Sofyan, University of Szeged, Tel : +36 20 392 2897, akhmad.sofyan@geo.u-szeged.hu

Received: 25.05.2023 Accepted: 16.07.2023

Abstract - Well "X" is one of the geothermal production wells, which produces two-phase fluids which are steam and brine. The pressure of fluid flow from the reservoir to the surface can decrease, so the fluid flow patterns can change. Determination of the flow pattern is very necessary to estimate the depth of the flashing zone where the condition of steam escapes from liquid and it can cause the scale precipitation which can be a major issue in the decline of the production rate. Concerning that, a continuous pressure drop will cause a slug flow and it will cause the fluid flow to become turbulent (irregular). The aim of the current research were to identify the fluid flow pattern, to estimate the scaling accumulation zone, and to determine the scaling type in the well. The current research can be used as a guide to decide what steps should be taken to avoid and eliminate scaling problems. The fluid flow pattern was determined using the Hewitt-Robert method. The scaling accumulation zone was estimated by using the PTS (pressure, temperature, and spinner) survey data. The scaling type was determined through chemical analysis of the scaling rock collected from the wellbore. The new finding in this research results indicated that the fluid flow pattern conformed to the annular flow category as established through the Hewitt-Robert method and it can promote scaling precipitation. The future research of developing the cleansing method can be conducted in this location. In addition, the flashing zone was estimated at a depth of 4600 ft from a total depth up to 5000 ft. Based on the scaling rock mineral analysis results, it was validated that the scaling type was amorphous silica.

Keywords- Annular flow; Casing; Flashing Zone; Flow Pattern; Geothermal; Production.

1. Introduction

Since being covered by the Ring of Fire, Indonesia country has geothermal potential as proven by the country's 117 active volcanoes which are spread among the islands of Sumatra, Java, Maluku, Nusa Tenggara, and Sulawesi [1]. Geothermal potential in Indonesia is estimated at around 29,51 MW. Nevertheless, just 4.5% of it is used for electricity in the nation. In this world, the highest geothermal energy potential is found in Indonesia, which accounts for around 40% of global potential [2]. With a goal of 7.2 GW in

2025 and 17.6 GW in 2050, the government is still working to expand the geothermal power plants [3].

Geothermal can be interpreted as energy generated from the earth, which is a combination of the Greek terms geo (earth) and thermal (heat). The energy is contained in geothermal fluids in the form of steam, liquid or both as a mixture [1]. The geothermal power plant produces electricity from geothermal energy. The geothermal power plant is called as a renewable, sustainable, and eco-friendly generator because of the characteristics of the geothermal energy [4]. In addition, Geothermal energy has its limitations, as Radek

explains that it can only be produced at specific times, requires reservation, and is not universally available [5]. In contrast, Pedro Angumba presents a more positive outlook, highlighting geothermal energy as a renewable source that remains accessible throughout the year [6]. Recognizing its potential, Syed Zafar emphasizes the need for comprehensive investigation and discovery of geothermal energies [7]. Additionally, Abdelkader Harrouz highlighted that geothermal energy represents an opportunity to meet the needs of future generations [8].

Along with the rapid demand for energy consumption due to changes in lifestyle and population growth [9], geothermal energy production, as one of the alternative energies, must be improved to meet the 2025 national energy target. Development of geothermal energy involves several processes, including (1) the preliminary survey of 3G (geology, geochemistry, and geophysics), (2) the exploration survey of 3G, (3) the exploration drilling, (4) the project review and planning, (5) the field development, (6) the power plant construction, (7) commissioning, and (8) operation [10].

The process of utilizing geothermal energy involves the extraction of geothermal fluid from subsurface reservoirs which contains heat energy. Then the geothermal fluid is converted into electricity. This fluid comes from a layer of a geothermal reservoir, which is created when heat is transferred from a heat source to the surrounding rocks, facilitated by both conductive and convective processes [11].

Given the unique composition and varying rock properties of each reservoir layer in the earth, it is imperative to conduct thorough research to identify effective strategies for addressing site-specific issues. In the context of extracting geothermal energy from deep wells, one of the most common challenges faced is the impact of the geothermal fluid's chemical properties. The fluid often contains minerals and gases in high concentrations, which can result in scaling and corrosion within the wells and surface infrastructure [12].

Scaling is the process of deposit or solid formation along the flow pipe during the production of geothermal energy as a result of temperature, pH, and pressure changes in a liquid system. Meanwhile, the chemical composition of the liquid has a significant impact on the type of scaling. The scaling accumulation zone and its underlying cause can be estimated by examining the fluid flow pattern as well as the properties of the fluid and scaling rock obtained from the geothermal wells [13].

Scaling is a common issue in the casing series of geothermal wells. The blockages caused by scaling in the well can significantly impede the production of geothermal energy. Therefore, it is very important to conduct an in-depth analysis of the scaling accumulation zone and fluid flow patterns within the well to ascertain the root causes of the reduced geothermal energy production [14]. The in-depth analysis can provide valuable insights for devising effective strategies to avoid and remediate scaling-related issues in the wells, thereby optimizing the efficiency and sustainability of geothermal energy production.

This study was conducted at the Salak field geothermal system, which is connected to multiple volcanic eruption centres near Indonesia's Mount Salak. The geothermal manifestations in the area are fumaroles and sulphate hot springs, which are strongly associated with the geothermal system, whereas bicarbonate hot springs and bicarbonate-chloride mixed springs are found at lower elevations.

The Salak geothermal field has 110 wells including 77 production wells, 10 injection wells (condensate), 12 injection wells (brine), 6 abandon wells, and 5 monitoring wells, resulting in an electricity capacity of 377 MW. The geothermal generation system used in the Salak geothermal field is a separated steam cycle consisting of Power Generation Facilities (PGF) and Resource Production Facilities (RPF) [15].

In 2015, two studies were conducted to investigate different aspects of fluid flow patterns in geothermal wells. In the first study, which was carried out in Banjarmasin, the effects of salt concentrations on the two-phase fluid (gas-liquid) flow were investigated. The Hewitt-Robert method was utilized for mapping the flow pattern. This first study aimed to determine the fluid flow patterns and found that the pattern was annular before flooding and churn during flooding [16]. Furthermore, In the second study, which was conducted by Flores Armenta in the same year, the WellSim software was utilized to investigate the thermodynamic state and flow pattern of the geothermal fluid at different depths in the wellbore. This second study aimed to investigate the causes of production decline and improve the efficiency of geothermal energy production [17]. Furthermore, Tolivia's research in 1972 reported that flow pattern analysis can predict the scaling formation in geothermal wells since the scaling can significantly reduce production efficiency [18]. Collectively, these studies demonstrate the importance of fluid flow pattern analysis in optimizing geothermal energy production and preventing scaling-related problems in the wellbore.

Scaling mainly can occur in a well in two forms which are silica scaling and calcite scaling. At high temperatures, the silica in the rock will dissolve in the liquid, then evaporate and then precipitate on the casing wall. However, calcite in the rock does not dissolve in liquid and instead loses carbon dioxide, converting to calcium carbonate due to a decrease in pressure. These scaling phenomena take place in the annular flow zone and along the wellbore. Previous studies by Widodo et al. in 2015 [16] and Tolivia in 1972 [18] did not use field data and did not determine the specific flow pattern that can lead to scaling. Similarly, Flores Armenta et al. (2015) identified flow patterns but did not determine which patterns could cause scaling [17]. In 2020, Zolfagharroshan and Khamehchi predicted scale precipitation and deposition during drilling but did not address the flow pattern responsible for scaling. Therefore, new research is necessary to fill these gaps in knowledge [19].

This research had four main objectives which were (1) to identify the fluid flow patterns in the well "X" using the Hewitt-Robert calculation method, (2) to estimate the scaling accumulation zone in the well through the analysis of the

Pressure, Temperature, and Spinner (PTS) survey data, (3) to identify the specific fluid flow pattern that could cause scaling, (4) to validate the type of scaling in the well through the chemical analysis of scaling rock obtained from the geothermal wellbore of the well "X".

2. Geological Background

In the West Java province, Indonesia, near the Sunda Volcanic Arc, there is a geothermal field of Salak (also known as Awibengkok) (Fig.1). It is encircled by mountains which range in elevation of 950 - 1,500 metres above sea level. The distance of the Salak geothermal field from Jakarta (the capital city of Indonesia) is around 60 kilometres.

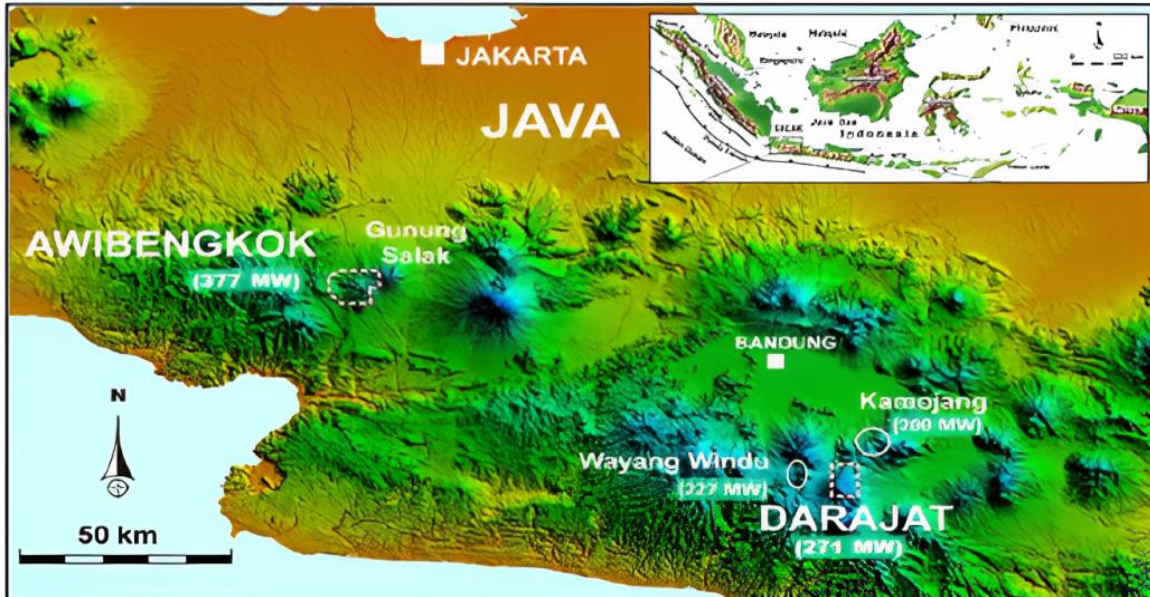


Fig.1. Position of the Awibengkok/Salak geothermal field [15].

The salak geothermal system is mostly liquid and has a fracture-controlled reservoir that has moderate to high temperatures ranging from 464°F to 600°F. The system contains benign fluids with moderate to low non-condensable gas. This geothermal reservoir is connected to recent volcanic activities and intrusions in the highlands region east of the Cianten caldera and west of Salak mountain [20].

The recent volcanic vent systems are concentrated along the Cibereum and Awi faults, which predominantly trend in a north-to-northeast direction with subsidiary northwest and east-west trends. The ancestral andesitic cone that created the edge of the Cianten Caldera to the west was active around 1610 to 670 ka, while the significant peaks of the Salak area were formed between 860 and 180 ka (Fig. 2).

The Salak geothermal production region has andesite, rhyodacite and lavas that date back from 185 to 280 ka. These are overlain by lavas, rhyolitic domes, and related tephra sequences, which are primarily erupted along a fault trending in a north-northeast direction. The rhyolitic volcanism's age is between 120 and 40 ka based on K-Ar and 40Ar/39Ar dating.

At the top, the system has an extensive tephra known as the "Orange Tuff" which dates back between 40,000 and 8400 years before the present (B.P.) according to Stimac et al. (2008). This is bracketed by 14C dates on underlying lahar and overlying hydrothermal breccia units.

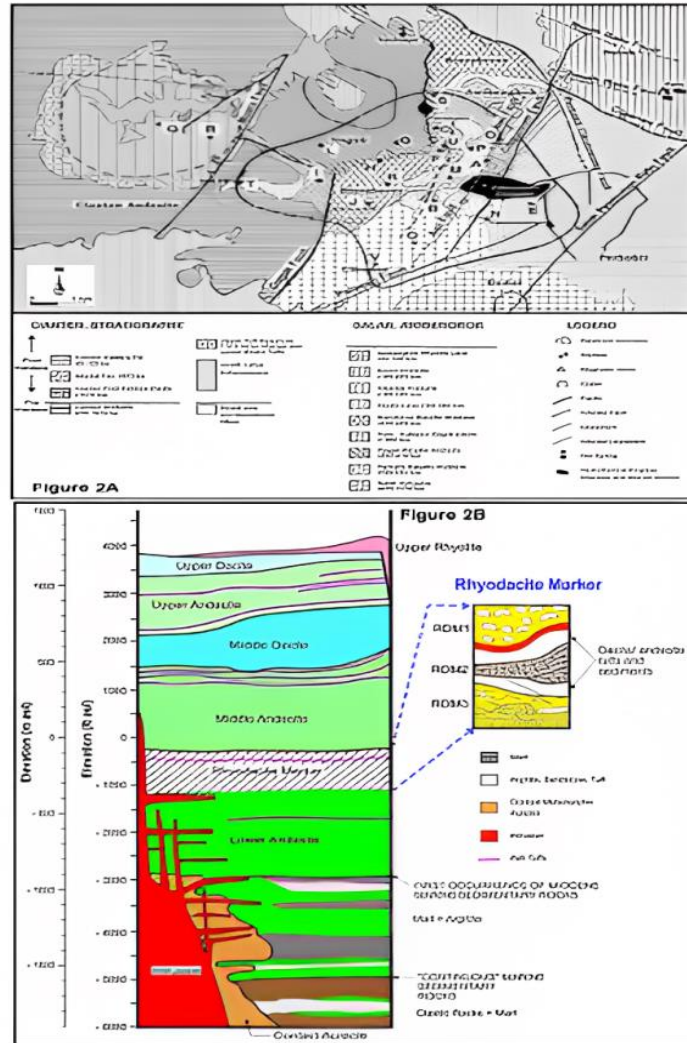


Fig. 2. (A) Major rock types, prominent faults, altered ground, current reservoir boundary and well Pad locations of Surface geology of the Salak area, and (B) Representative stratigraphic column for the Awibengkok reservoir. Source : [20].

The geothermal reservoir is mainly located within a sequence of volcanic rocks ranging from andesite to rhyodacite. These rocks are underlain by marine sedimentary rocks from the Miocene era, and both types of rocks have been intruded by igneous formations [15]. The stratigraphic section can be classified into four big formations that correspond to different stages in the evolution of the Sunda Volcanic Arc in western Java.

- The first formation is made up of shallow-marine carbonates and sedimentary rocks.
- The second formation is the Lower Volcanic Formation which consists of andesitic to basaltic volcanic rocks interbedded with sedimentary rocks.
- The third formation is the Middle Volcanic Formation which includes andesitic-to-dacitic lavas, tuffs, lahars, and debris flows. This formation represents the construction, collapse, and erosion of stratovolcanoes

and lava dome complexes. This formation also contains silicic rock that represents a period of silicic volcanism and caldera formation.

- The fourth formation is the Upper Volcanic Formation which includes another andesitic sequence overlain by dacitic to rhyolitic rocks, including the surface deposits described earlier.

Each major volcanic formation can be divided into a lower andesitic section and an overlying rhyolitic or dacitic section, representing distinct or partially overlapping volcanic episodes that have become progressively more silicic over time (Fig. 2).

3. Method

The detailed flow chart of this research is presented in Fig. 3.

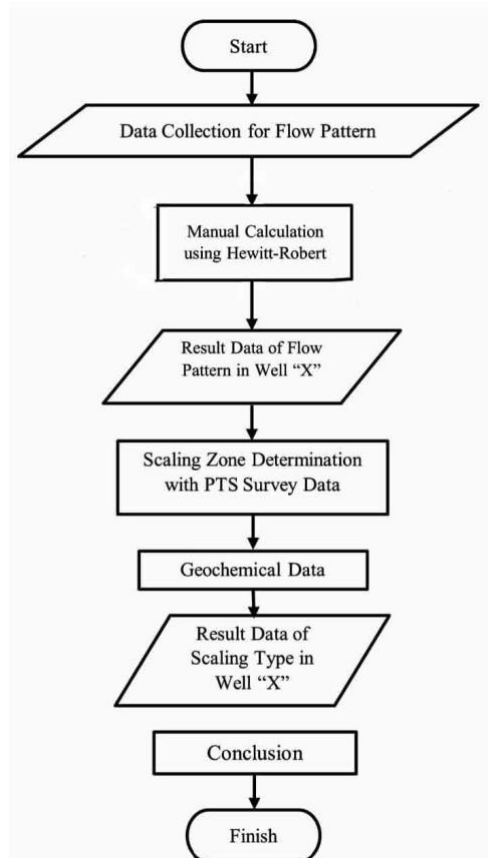


Fig. 3. Flowchart of the research

The research utilized data which were collected from the well “X” in the Salak geothermal field. The data include chemical analysis results of the scaling rock, data of the PTS survey, data of well production, data of wellhead pressure, data of well profile, data of flow rate, and data of casing/piping. After all necessary data had been collected, the data were then analysed to determine the flow pattern using the manual calculation following the Hewitt-Robert method. In addition, the PTS survey data were used to determine the flashing zone's depth, which provided insight into the accumulation zone of scaling in well production casing of well “X”. By identifying the location of the flashing zone, it is possible to estimate the depth at which scaling occurs due to changes in temperature, pH, and pressure in the fluid [21]. After that, the chemical analysis of scaling rock was conducted to identify the type of scaling. This step was crucial in providing concrete evidence of scaling's existence in the well “X”, as it confirmed that scaling was occurring in the specific flashing zone and flow pattern that had been identified earlier.

a. The Hewitt-Robert Method

Flow pattern or flow area is one of the important parameters for classifying two-phase fluid flow. Flow pattern specifications are based on the shape or type of flow distribution which generally occurs due to the effects of viscosity, density or surface tension. The determination of vertical flow patterns is currently accomplished through the

widely accepted application of logarithmic graphs proposed by Fair (1960) and Hewitt and Roberts (1969) in the field [22].

The flow pattern of fluid in this study was determined manually through the Hewitt-Robert method. This calculation required several data including depth, pressure, enthalpy, flow rate, pipe dryness, and pipe diameter. The pipe cross-sectional area (A_p) of the well “X” was calculated using a formula according to the Hewitt-Robert method that include the parameter of constant (3.24) value and the diameter of the inside of the casing (m). The resulting coordinates of the X and Y flow patterns were then used to determine the actual flow pattern in the well “X”.

b. The collection and chemical analysis of scaling rock sample

The Obstruction Identification were conducted to prove the scaling deposition in the wellbore using the Impression Block method. The tools were lowered down along the wellbore and stuck in the depth of 2,630 - 4,734 ft MD with a white stamp trace on the surface of the Impression block. This sign indicated the occurrence of scaling deposition in the wellbore as shown in Fig. 4.

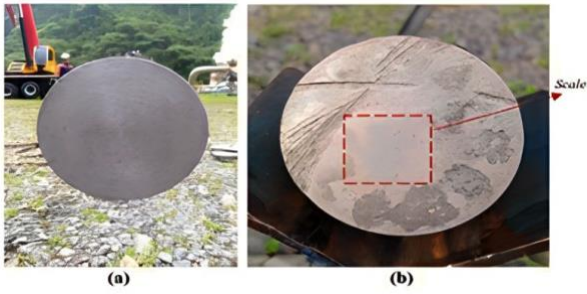


Fig. 4. (a) Impression block before use and (b) After use with white stamp

The scaling rock sample was collected from the production liner casing using a sample catcher in the wellbore and then brought to the laboratory for the mineralogical composition analysis. The identification of the main and accessory mineral contents in the samples was carried out through X-ray powder diffraction (XRD) analysis using a Panalytical X'Pert Pro diffractometer with Cu-K α

radiation ($\lambda = 1.54598 \text{ \AA}$). Before analysis, the samples were milled in an agate mortar to create powders [23]. The powders were then treated with a 2N HCl solution to remove the carbonate fraction. Furthermore, the sample was suspended in ethanol and loaded onto silica plates. Then, the ethanol was evaporated. The XRD analysis was conducted repeatedly. The Panalytical software "High Score Plus" was used to analyse the diffractograms and identify the minerals.

4. Results and Discussions

a. The Well "X" Profile

The well "X" is located in Salak geothermal field. The well is a water-dominated well having a depth up to 5000 ft and producing an energy capacity of 15 MW. As seen in Fig. 5, the well "X" has 20" and 13 3/8" production casings and 10 3/4" production liners.

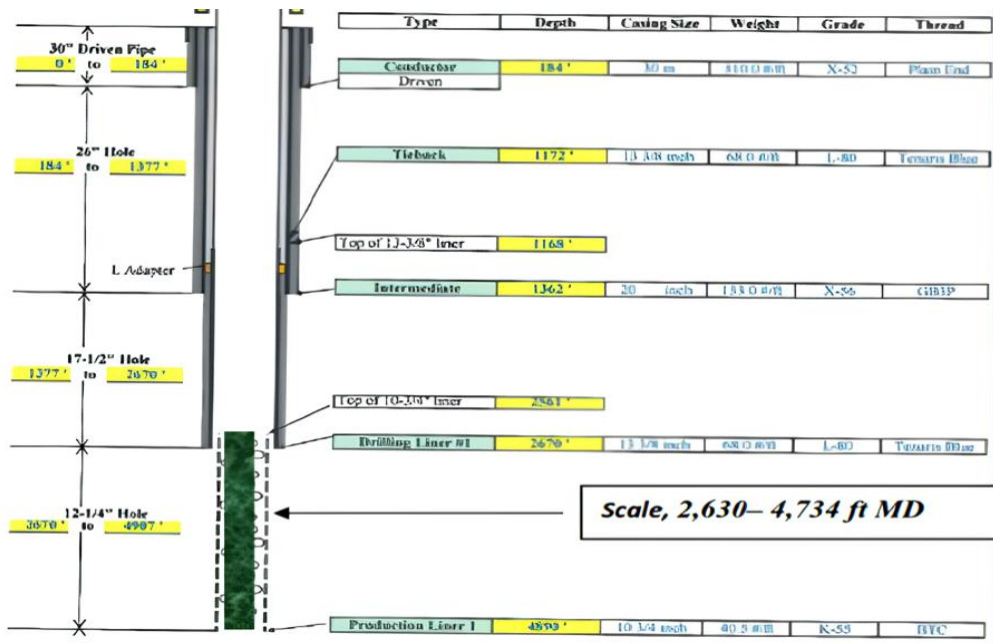


Fig. 5. Profile of the Well "X"

b. Determination of Fluid Flow Pattern

The Hewitt-Robert calculation method was used to find the vertical fluid flow pattern in the well "X" because the hot water and steam fluid flows move upward (vertically up flow) having a pressure range from atmospheric pressure to 1000 psi [21]. The following are the procedures for determining the vertical flow pattern:

i. Calculation of the cross-sectional area

The cross-sectional area of the flow pipe (A_p) which is calculated in this sub-section 4.2.1 is the cross-sectional

area of the casing before the wellhead, which is the 13 3/8" production casing having an inner diameter of 7.025 inches. The A_p was calculated through the Equation (1).

$$A_p = \pi \frac{di^2}{4} \tag{1}$$

$$A_p = 3.14 \frac{(7.025 \times 0.0254)^2}{4}$$

$$A_p = 0.025 \text{ m}^2$$

Where:

A_p = the flow pipe's cross-sectional area (m^2)

π = the constant (3.24)

d_i = The diameter of the inside of the casing (m)

Therefore, based on these calculations, the flow pipe’s cross-sectional area in the Well “X” was 0.025 m².

ii. Calculation of the coordinates of the flow pattern map

In this sub-sub-section 4.2.2, Equations (2) and (3) were used to determine the coordinates (X, Y) of the flow pattern map [22]. For example, the surface of the well “X” was known to have a dryness (q) = 0.2309, a total mass flow (M_{total}) = 3.7295 kg/s, a cross-sectional area (A_p) = 0.025 m², a water density (ρ_l) = 898.0645 kg/m³ and a vapour density (ρ_g) = 4.0656 kg/m³. Hence, the coordinates (X, Y) can be calculated by the following:

$$X \text{ Axis} = \frac{Gl^2}{\rho_l} = \frac{\left(\frac{(1-x)M_{total}}{A_p}\right)^2}{\rho_l} \quad (2)$$

$$X \text{ Axis} = \frac{Gl^2}{\rho_l} = \frac{\left(\frac{(1-0.2309)3.7295}{0.025}\right)^2}{898.0645}$$

$$X \text{ Axis} = 14.64 \text{ kg/ms}^2$$

$$Y \text{ Axis} = \frac{Gg^2}{\rho_g} = \frac{\left(\frac{(1-2309)3.7295}{0.02502}\right)^2}{4.0656} \quad (3)$$

$$Y \text{ Axis} = 291.3447 \text{ kg/ms}^2$$

Where:

$Y\text{-axis}$ = vertical axis (kg/(ms²))

$X\text{-axis}$ = horizontal axis (kg/(ms²))

Gg = mass flux of gas phase flowing alone in the channel (kgm⁻²s⁻¹)

Gl = mass flux of liquid phase flowing alone in the channel (kgm⁻²s⁻¹)

ρ_g = gas density (kg/m³)

ρ_l = liquid density (kg/m³)

q = dryness

A_p = the cross-sectional area (m²)

M_{total} = total mass (kg/s)

By the same calculation way, the coordinates (X, Y) at various Wellhead pressures in the well “X” was determined and presented in Table 1.

Table 1. Results of Determination of the X and Y axis of the Hewwit-Robert’s plot

WHP (Well Head Pressure)			Wellhead Enthalpy			Wellhead	Mass Flow		A_p	Water	Steam		
			Total (hWH)	Liquid (hfWH)	Vapor (hgWH)	Dryness	Total	Density (ρ_l)			Axis X (Gl^2/ρ_l)	Density (ρ_g)	Axis Y (Gg^2/ρ_g)
psig	psia	bara	kJ/kg	kJ/kg	kJ/kg	(xWH)	Ton/hour	kg/s	m ²	kg/m ³	kg/(ms ²)	kg/m ³	kg/(ms ²)
103	114.76	7.81	1190	716.59	2767.3	0.2309	13.42633	3.7295	0.02502	898.0645	14.6411	4.0656	291.3447
103	114.76	7.81	1190	716.59	2767.3	0.2309	14.65103	4.0697	0.02502	898.0645	17.4339	4.0656	346.9196
105	116.76	7.94	1190	719.72	2768.01	0.2296	13.60777	3.7799	0.02502	897.3356	15.1008	4.1328	291.2149
106	117.76	8.01	1190	721.26	2768.36	0.229	13.33562	3.7043	0.02502	896.9739	14.5321	4.1664	275.9271
107	118.76	8.08	1190	722.8	2768.7	0.2284	13.29026	3.6917	0.02502	896.6141	14.4623	4.1999	270.3955
103	114.76	7.81	1190	716.59	2767.3	0.2309	13.2449	3.6791	0.02502	898.0645	14.248	4.0656	283.5238
106	117.76	8.01	1190	721.26	2768.36	0.229	12.11092	3.3641	0.02502	896.9739	11.9855	4.1664	227.5738
106	117.76	8.01	1190	721.26	2768.36	0.229	10.93158	3.0365	0.02502	896.9739	9.7649	4.1664	185.4103
105	116.76	7.94	1190	719.72	2768.01	0.2296	11.52125	3.2003	0.02502	897.3356	10.8249	4.1328	208.7558
105	116.76	7.94	1190	719.72	2768.01	0.2296	17.64474	4.9013	0.02502	897.3356	25.3896	4.1328	489.6325

The Hewitt-Robert flow pattern mapping method is useful in determining the vertical flow pattern in well "X" by analysing the behaviour of steam and hot water moving upward under pressures ranging from atmospheric pressure up to 1000 psi. The Hewitt-Robert flow pattern graph provides a visual representation of the flow pattern type by plotting the X and Y-axis parameters. Six types of flow

pattern behaviours frequently seen in geothermal wells are "annular", "wispy annular", "bubbly", "bubbly-slug", "slug", and "churn". By plotting the X-axis and Y-axis values (showed in Table 1) on the flow pattern graph, the point of intersection of the X-Y axis and the line of the annular flow pattern is discovered (see Fig. 6). Then, the type of flow patterns at various wellhead pressures is shown in Table 2.

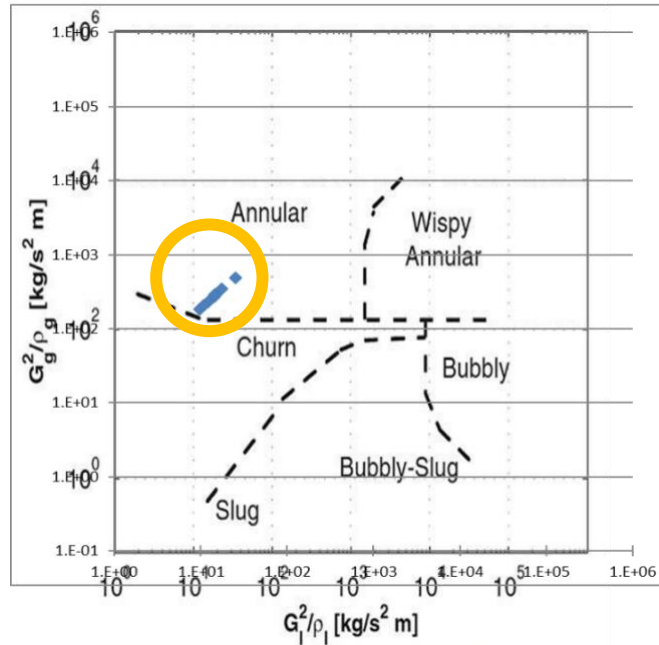


Fig. 6. Plotting the coordinates values on the Hewitt-Robert Flow Pattern Graph

Table 2. The Type of Vertical Flow Patterns based on Hewitt Roberts Method

WHP (Well Head Pressure)			X Axis ($G1^2/\rho1$)	Y Axis ($Gg^2/\rho g$)	Flow Pattern
psig	psia	Bara	kg/(ms ²)	kg/(ms ²)	
103	114.76	7.8068027	14.64107106	291.344736	(Annular)
103	114.76	7.8068027	17.4338968	346.9195691	(Annular)
105	116.76	7.9428571	15.10079162	291.2148845	(Annular)
106	117.76	8.0108844	14.53207693	275.9271044	(Annular)
107	118.76	8.0789116	14.46234854	270.3954626	(Annular)
103	114.76	7.8068027	14.24804011	283.5237579	(Annular)
106	117.76	8.0108844	11.98548328	227.5737811	(Annular)
106	117.76	8.0108844	9.764884544	185.4102706	(Annular)
105	116.76	7.9428571	10.82491858	208.7557721	(Annular)
105	116.76	7.9428571	25.38963209	489.6325282	(Annular)

Based on the analysis of the flow pattern in well "X" at various wellhead pressures as shown in Fig. 4 and Table 2, it can be inferred that the flow pattern observed is an annular flow pattern, which leads to an increased vapour fraction for

all types of wellhead pressures. An annular flow pattern is characterized by fluid flowing in the internal perimeter of the channel in which the gas or vapour has a higher velocity at the centre. The annular flow pattern is regarded as the ideal

flow pattern in piping systems since it is relatively stable [24]. In well "X," the observed flow pattern is an annular flow pattern with a vapour fraction of 100%. This flow pattern is highly desirable as it results in the highest vapour fraction, making it capable of producing large amounts of steam. Moreover, annular flow is known for its stability and safety, making it a preferred choice compared to turbulent flow patterns that can cause irregular flow and significant friction [25].

c. *Determination of the flashing zone depth*

One of the various geothermal well monitoring procedures that are frequently used to describe the flow along the wellbore is the pressure, temperature, and spinner (PTS) survey [26].

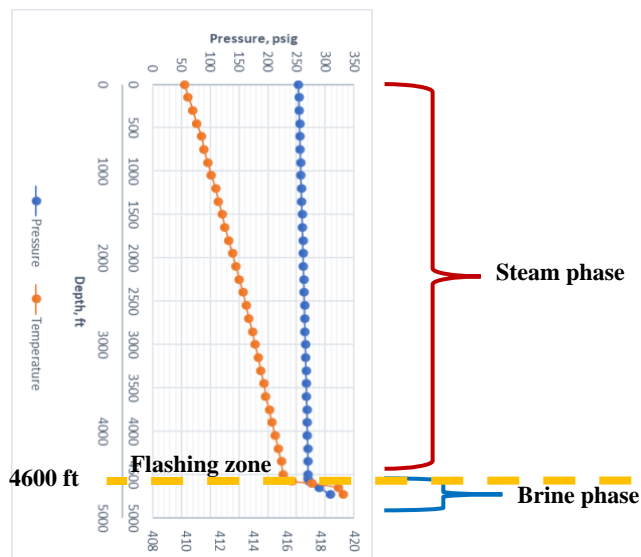


Fig. 7. Pressure and Temperature Survey data at Well "X"

Based on Fig. 7, it indicates that the well "X" is a production well that primarily produces steam fluid. The pressure (shown in blue color) steadily increases throughout the production casings, from a depth of 4600 ft to the surface of the well "X" (Fig. 7). This indicates that there is no brine flow which could cause pressure fluctuations.

However, at depths of 4600 ft to 4800 ft, there is a sudden change in pressure and temperature (Fig. 7), indicating the presence of brine flow at these depths. The flashing zone is predicted to be at a depth of 4600 ft, where there is a pressure drop from 418.5 psig to 416.5 psig because of a difference in diameter of the perforated liner (having a smaller diameter of 7.025 inches) with that of the production casing (having a larger diameter of 13 3/8 inches). This pressure drop results in the release of steam from the brine, a phenomenon referred to as flashing. As a result, the steam fluid that reaches the surface has a high vapour fraction.

The process of flashing in the well "X" has a significant effect on the composition of the brine. When the pressure and temperature decrease during flashing, some of the water in the brine turns into steam, resulting in a higher concentration of scaling compounds. Additionally, the release of gases like CO₂ and H₂S alters the brine pH and increases ion concentrations. These changes can contribute to the scaling formation in the well "X", which can negatively affect its productivity and longevity [27]. Therefore, the

steam fluid will move more quickly after the flashing area reaches the surface [21].

d. *Determination of the scaling type*

In order to ensure a sustained steam production from the well "X", identification of the type of scaling that is formed in the formation and around the liner is crucial. Based on the PTS analysis (sub-section 4.3), there is the presence of a flashing zone that can contribute to scaling. This is due to the drop in pressure and temperature, which results in the release of H₂S and CO₂ gases, thus affecting the pH of the brine. Therefore, it is essential to confirm the type of scaling formed in the well "X" to prevent a decrease in steam production over time.

Table 3. The results of the chemical analysis of the scaling sample obtained from the well "X"

Element	Well X
Quartz (SiO ₂)	10
Magnetite (Fe, Mg, Zn, Cu, Ni)(Fe, Al, Cr)2O ₄	12
Analcime (NaSi ₂ AlO ₆ .H ₂ O)	25
Plagioclase feldspar (Na, Ca)Al(Si,Al)3O ₈	<3
K-Feldspar KAlSi ₃ O ₈	<3
Pyrite FeS ₂	<5
Amorphous	>40
Unidentified	<5

The scaling sample was analysed in the laboratory to determine the mineralogical composition of the sample. The chemical compositions of the sample is presented in Table 3.

Based on the chemical analysis results, the scaling in the well "X" contained primarily amorphous silica material with a weight percentage of greater than 40% (see Table 3). Amorphous silica will form more readily than other silica types at lower temperatures [28].

A previous study by Zolfagharroshan and Khamsehchi [19] only focused on predicting the scale deposition and modelling the production of the energy using the HOLA software without providing a thorough explanation of the flow pattern associated with scaling in geothermal wells. This study, on the other hand, identified scaling zones and investigated the root causes of scaling by analysing the flow pattern, fluid characteristics, flashing zones, and chemical composition of the scaling rock in the well "X".

5. Conclusion

The conclusions derived from this research are outlined as follows:

- a) The analysis of well "X" indicates that the flow pattern formed along the casing series is classified as annular, as determined by Hewitt-Robert calculations.
- b) The potential for scaling in well "X" aligns with the identified flow pattern. In the annular flow zone, scaling may occur, with scaling accumulation increasing as the fluid boils on the casing wall.
- c) The estimated scaling accumulation zone is located at a depth of 4600 ft, between the casing shoe slotted liners of 7" and 13 3/8".
- d) Chemical analysis performed on the scaling sample obtained from well "X" confirms that the scaling type is amorphous silica.
- e) This study focuses on determining the flow pattern responsible for scaling and estimating the depth of the flashing zone. To further advance this research, future studies should prioritize the development of methods to prevent and remove scaling within the wellbore. Additionally, these methods should consider the financial and developmental aspects to achieve more effective and efficient results.

Acknowledgement

The authors would like to sincerely acknowledge all people who have supported the writing of this paper.

Funding

There is no funding for this study.

Conflict of Interest

The authors declared no conflict of interest in this manuscript.

References

1. Nasruddin, M.I. Alhamid, Y. Daud, A. Surachman, A. Sugiyono, H. B. Aditya, and T. M. I. Mahlia, "Potential of geothermal energy for electricity generation in Indonesia: A review." *Renewable and Sustainable Energy Reviews*, Vol. 53, No. 2016, 2016, 733–740. <https://doi.org/10.1016/j.rser.2015.09.032>. (Article)
2. A. Sofyan, Y. Dwi, G. Bujang, and D. C. Dewi, "Analysis of The Z Well Production Test Using The Horizontal LIP Pressure Method at PT. Pertamina Geothermal Energy Ulubelu Area." *Indonesian Journal of Energy and Mineral*, Vol. 3, No. 1, 2023, 40–55.(Article)
3. Dewan Energi Nasional Republik Indonesia, "Geothermal: The Sustainable Energy For Green Recovery, Energy Transition, And Security." *DEN Annual Publication*. Retrieved April 21, 2023, from <https://den.go.id/index.php/dinamispage/index/1332-geothermal-the-sustainable-energy-for-green-recovery-energy-transition-and-security.html> ((Standards and Reports)
4. A. Holm, D. Jennejohn, and L. Blodgett, "Geothermal Energy and Greenhouse Gas Emissions Two new geothermal power plants in California: EnergySource's John L. Featherstone Plant (top) and Ormat's North Brawley Plant. 2 Geothermal Energy and Greenhouse Gas Emissions," No. November, 2012. (Standards and Reports)
5. R. Byrtus, R. Hercik, J. Dohnal, J. B. Martinkauppi, T. Rauta, and J. Koziorek, "Low-power Renewable Possibilities for Geothermal IoT Monitoring Systems." *11th IEEE International Conference on Renewable Energy Research and Applications, ICRERA 2022*, 2022, 164–168. <https://doi.org/10.1109/ICRERA55966.2022.9922835> (Conference Paper)
6. P. Angumba, A. Cardenas, and D. Icaza, "Geothermal and Solar Energy Applied to Air Conditioning and Electricity Generation for Homes: Case study Baños in Cuenca-Ecuador." *10th International Conference on Smart Grid, icSmartGrid 2022*, 2022, 407–413. <https://doi.org/10.1109/icSmartGrid55722.2022.9848548> (Conference Paper)
7. S. Z. Ilyas, "Review of the renewable energy status and prospects in Pakistan." *International Journal of Smart grid*, Vol. 5, No. 4, 2021. <https://doi.org/10.20508/ijsmartgrid.v5i4.220.g174> (Article)
8. A. Harrouz, A. Temmam, and M. Abbes, "Renewable Energy in Algeria and Energy Management Systems." *International Journal of Smart grid*, Vol. 2, No. 1, 2017. <https://doi.org/10.20508/ijsmartgrid.v2i1.10.g9> (Article)

9. M. E. Shayan, "The Biomass Supply Chain Network Auto-Regressive Moving Average Algorithm." *International Journal of Smart grid*, Vol. 5, No. 1, 2021. <https://doi.org/10.20508/ijsmartgrid.v5i1.153.g135> (Article)
10. I. G. Association, "Best Practices Guide for Geothermal Exploration." *IGA Service GmbH, Bochum Germany*, 2014. (Standards and Reports)
11. N. M. Saptadji, *Teknik panasbumi*. Bandung: ITB University Press. (Book)
12. E. Gunnlaugsson, H. Ármannsson, S. Thorhallsson, and B. Steingrímsson, Problems in geothermal operation-scaling and corrosion. *Short Course VI on Utilization of Low-and Medium-Enthalpy Geothermal Resources and Financial Aspects of Utilization*. Santa Tecla. (Book)
13. C. Sapto, and P. Salvius, *Evaluasi Potensi Silica Scaling Pada Pipa Produksi Lapangan Panasbumi Lahendong – Sulawesi Utara*. Yogyakarta: Yogyakarta. (Standards and Reports)
14. E. T. S. Agustinus, I. Syafri, M. F. Rosana, and I. Zulkarnain, "Scale Prevention Technique to Minimized Scaling on Re-Injection Pipes in Dieng Geothermal Field, Central Java Province, Indonesia." *Indonesian Journal on Geoscience*, Vol. 5, No. 2, 2018. <https://doi.org/10.17014/ijog.5.2.129-136> (Article)
15. N. Ganefianto, J. Stimac, L. Sirad-Azwar, R. Pasikki, M. Parini, E. Shidartha, A. Joeristanto, G. Nordquist, and K. Riedel, "Optimizing Production at Salak Geothermal Field, Indonesia, Through Injection Management." *Proceedings World Geothermal Congress*, No. April, (2010), 25–29. Retrieved from <https://www.geothermal-energy.org/pdf/IGASTandard/WGC/2010/2415.pdf> (Conference Paper)
16. E. Widodo, A. Akbar, and J. Timur, *Pengaruh Konsentrasi Garam Terhadap Karakteristik Aliran Dua Fase Gas Dan Air*. Universitas Muhammadiyah Sidoarjo. (Book)
17. A. M. Flores, M. M. Ramírez, and A. A. V. L. Morales "Wellbore Modeling of Production Well H-1D using WellSim, Los Humeros Geothermal Field, México." *Proceedings World Geothermal Congress*, No. April, (2015), 19–25. (Conference Paper)
18. E. Tolivia, "Flow in geothermal wells (An analytical study)." *Geothermics*, Vol. 1, No. 4, 1972, 141–145. [https://doi.org/10.1016/0375-6505\(72\)90023-5](https://doi.org/10.1016/0375-6505(72)90023-5) (Article)
19. M. Zolfagharroshan, and E. Khamsehchi, "A rigorous approach to scale formation and deposition modelling in geothermal wellbores." *Geothermics*, Vol. 87, No. March, 2020, 101841. <https://doi.org/10.1016/j.geothermics.2020.101841> (Article)
20. D. Yudha, S. Sarulla, O. Limited, N. V. Aprilina, D. Y. Satya, S. Rejeki, G. Golla, and M. Waite, "Geologic Modeling Workflow for Volcanic Hosted Geothermal Reservoirs: Case Study from Salak Geothermal Field 3D Earth Modeling View project Salak 3D Static Modeling View project Geologic Modeling Workflow for Volcanic Hosted Geothermal Reservoirs: Case St." *Proceedings World Geothermal Congress*, No. June 2016, 2015, 19–25. Retrieved from <https://www.researchgate.net/publication/304471645> (Conference Paper)
21. A. Sofyan, S. Wiharti, J. Szanyi, B. Y. Suranta, and R. Njeru, "Determination of Scaling Zone and Scaling Type in Slotted Liner Based on the Fluid Flow Pattern in the Geothermal Well 'X.'" *International Journal of Renewable Energy Research*, Vol. 13, No. 1, 2023, 276–286. <https://doi.org/10.20508/ijrer.v13i1.13603.g8681> (Article)
22. J. R. Thome, "Engineering Data Book III: Enhanced heat transfer design methods for tubular heat exchangers," 2016. (Book)
23. C. Wanner, F. Eichinger, T. Jahrfeld, and L. W. Diamond, "Causes of abundant calcite scaling in geothermal wells in the Bavarian Molasse Basin, Southern Germany." *Geothermics*, Vol. 70, No. November 2016, 2017, 324–338. <https://doi.org/10.1016/j.geothermics.2017.05.001> (Article)
24. J. R. Thome, , and A. Cioncolini, *Two-Phase Flow Pattern Maps for Microchannels*. https://doi.org/10.1142/9789814623216_0020 (Book)
25. T. Ganat, and M. Hrairi, "Effect of flow patterns on two-phase flow rate in vertical pipes." *Journal of Advanced Research in Fluid Mechanics and Thermal Sciences*, Vol. 55, No. 2, 2019, 150–160. (Article)
26. Herianto. "Analisis Data Pressure Temperature Spinner Untuk Penentuan Potensi Sumur Panas Bumi 'RB-1' Lapangan Kerinci," 2019, 9–25. (Standards and Reports)
27. Solenis. "Cutting-Edge Scale Control Solutions For Geothermal Power Producers (EMEA And APAC)." *Solenis.com*. Retrieved September 18, 2021, from <https://www.solenis.com/en/resources/events/webinars/cutting-edge-scale-control-solutions-for-geothermal-power-producers-emea-apac> (Webpage)
28. M. Tassew, "Effect of solid deposition on geothermal utilization and methods of control," No. 13, 2001, 1–20. (Book)